

Photocatalytic hydrogen generation from water under visible light using core/shell nano-catalysts

X. Wang, K. Shih and X. Y. Li

ABSTRACT

A microemulsion technique was employed to synthesize nano-sized photocatalysts with a core (CdS)/shell (ZnS) structure. The primary particles of the photocatalysts were around 10 nm, and the mean size of the catalyst clusters in water was about 100 nm. The band gaps of the catalysts ranged from 2.25 to 2.46 eV. The experiments of photocatalytic H₂ generation showed that the catalysts (CdS)_x/(ZnS)_{1-x} with *x* ranging from 0.1 to 1 were able to produce hydrogen from water photolysis under visible light. The catalyst with *x* = 0.9 had the highest rate of hydrogen production. The catalyst loading density also influenced the photo-hydrogen production rate, and the best catalyst concentration in water was 1 g L⁻¹. The stability of the nano-catalysts in terms of size, morphology and activity was satisfactory during an extended test period for a specific hydrogen production rate of 2.38 mmol g⁻¹ L⁻¹ h⁻¹ and a quantum yield of 16.1% under visible light (165 W Xe lamp, λ > 420 nm). The results demonstrate that the (CdS)/(ZnS) core/shell nano-particles are a novel photo-catalyst for renewable hydrogen generation from water under visible light. This is attributable to the large band-gap ZnS shell that separates the electron/hole pairs generated by the CdS core and hence reduces their recombinations.

Key words | core/shell structure, hydrogen generation, microemulsion, nano-photocatalyst, renewable energy, visible light

X. Wang
K. Shih
X. Y. Li (corresponding author)
Department of Civil Engineering,
The University of Hong Kong,
Pokfulam Road,
Pokfulam,
Hong Kong
E-mail: xiwang@hkusua.hku.hk;
kshih@hku.hk;
xlia@hkucc.hku.hk

INTRODUCTION

The global energy consumption has increased steadily in the past century, and fossil fuels supply about 86% of the world's energy today. However, fossil fuels are not renewable and their reserves are limited. More importantly, the combustion of fossil fuels emits greenhouse gases that largely contribute to the global warming problem. Thus, alternative energy sources are greatly needed. Hydrogen is considered as one of the most promising clean energy carriers in future. Hydrogen can be regenerated in a cyclic process from water. It has a high combustion value and a near-zero level of pollutant and greenhouse gas emissions.

Photocatalytic splitting of water is a promising and environmental-friendly method to harvest the solar energy for hydrogen generation (Fujishima & Honda 1972; Maeda *et al.* 2006). Visible light (λ > 420 nm) covers 43% of the

solar spectrum; however, only the catalysts with a great band gap is capable of splitting water with a sensible solar energy conversion efficiency (Ishikawa *et al.* 2003). Considerable efforts have been made on developing the photocatalysts that function under visible light, such as metal oxides, oxynitride and metal sulfides (Bak *et al.* 2002; Lee *et al.* 2007; Bao *et al.* 2008). However, the quantum yields of the visible-light-driven catalysts are rather low due to mainly the recombination of photo-generated electron/hole pairs. In recent years, metal sulfide co-catalysts have shown good photocatalytic activities under visible light (Tsuji *et al.* 2004, 2005; Zhang *et al.* 2007; Zong *et al.* 2008). However, the stability of the photocatalysts is still a concern for long-term applications. A core-shell co-catalyst structure can offer the benefit of integrated functions from two

doi: 10.2166/wst.2010.147

different catalyst materials. It allows tailoring the properties of the two materials with the shell layer to passivate the more active but less stable core material. This type of material structure has been recently used in solar cells and photochemistry (Law *et al.* 2006).

In the present development, the core-shell structure was adopted to fabricate the CdS-ZnS co-catalysts for photocatalytic hydrogen generation from water under visible light. While the small band-gap CdS has a high photocatalytic activity, the core (CdS) can be protected by the larger band-gap shell (ZnS) from corrosion in water (Yu *et al.* 2005). A microemulsion technique was used to prepare the nano-sized photocatalysts with different material combinations in a core-shell structure. The performance of the catalysts in photo-hydrogen generation from water splitting was determined, and the photophysical property, particle size and morphology of the catalysts were examined.

MATERIALS AND METHODS

Preparation and characterization of core-shell catalysts $(\text{CdS})_x/(\text{ZnS})_{1-x}$

The core-shell nano-catalysts were synthesized using the microemulsion method. All the chemicals and reagents were of analytical purity. Cadmium nitrate ($\text{Cd}(\text{NO}_3)_2$, 99%, Sigma-Aldrich) and Zinc nitrate ($\text{Zn}(\text{NO}_3)_2$, 99%, Sigma-Aldrich) were used as the Cd and Zn precursors. Sodium sulfide hydrate was purified by re-crystallization. A pure Cd microemulsion solution was prepared by adding a pre-determined amount of 0.1 M $\text{Cd}(\text{NO}_3)_2$ in an oil (W/O) microemulsion liquor consisting of hexane, butonal and Triton X100. A pure Zn microemulsion solution was also prepared by adding 0.1 M $\text{Zn}(\text{NO}_3)_2$ into the W/O liquor. An excessive amount of 0.1 M Na_2S was added in the same type of W/O liquor to form the Na_2S microemulsion. In making the catalysts, the $\text{Cd}(\text{NO}_3)_2$ microemulsion was added into the Na_2S microemulsion and the mixture was stirred for 15 min. The $\text{Zn}(\text{NO}_3)_2$ microemulsion was then added into the above solution and stirred strongly for 15 min. After ageing 12 h at room temperature, the solid catalysts were centrifuged and washed with deionized (DI)

water and pure alcohol, respectively. Finally, the yellow precipitates were dried at 50°C in vacuum for 6 h. The solids were ground thoroughly for 5 min, and the catalyst powders were kept in dark and dry condition before use. With different ratios of Cd and Zn used in the microemulsion procedure, a series of the catalyst compositions of $(\text{CdS})_x/(\text{ZnS})_{1-x}$ could be obtained with the ratio factor varying from 0.1 to 1.0.

In addition to photocatalytic hydrogen generation, the catalysts were characterized for their particle sizes, surface morphology and photo absorbance. The particle size distribution of the catalysts in water was measured by a laser diffraction particle size analyzer (LS13320, Beckman-Coulter). Prior to the measurement, the catalysts were dispersed and sonicated thoroughly in DI water. The diffuse reflection spectrum of the photocatalysts was obtained using a UV-vis Spectrophotometer (Lambda 25, Perkin Elmer) that was converted from the reflection function to the absorbance function according to the Kubelka-Munk method. The morphology of the catalysts was examined with a Leo 1530 scanning electron microscope (SEM). The transmission electron microscopic (TEM) images and electron diffraction (ED) patterns of the samples were obtained using a Philips Tecnai G2 20 S-TWIN microscope.

Photocatalytic activity measurement

The experiments of photocatalytic hydrogen evolution were performed in side irradiation cells with a volume of 72 ml each. The effective irradiation area for the cell was 53.43 cm². A pre-determined amount of the catalysts, e.g. 1 g/L, was dispersed into 60 ml of the solution that contained 0.2 M Na_2SO_3 and 0.1 M Na_2S as the electron donors in the cell. The catalysts were kept in suspension by water recirculation. The system was purged and saturated with nitrogen before sealed completely for the photocatalytic reaction. The photocatalysts were irradiated by visible light from a 100 W Hg lamp through a cut-off liquid filter ($\lambda > 420$ nm, $T = 92\%$). The amount of H_2 evolved was determined by a gas chromatography (Agilent 6850 Series II) with a thermal conductivity detector (TCD). Moreover, the effect of the catalyst load and the stability of the catalysts were evaluated at a higher visible light intensity from

a 165 W Xe lamp through a cut-off filter ($\lambda > 420$ nm, $T = 92\%$). The catalytic activity of the photocatalysts was evaluated based on the hydrogen production rate defined below by Equation (1) and the specific hydrogen production rate defined by Equation (2).

$$\text{Hydrogen production rate} = \frac{\text{moles of H}_2 \text{ evolution}}{\text{duration of reaction}}; \quad (1)$$

$$\begin{aligned} \text{Specific hydrogen production rate} \\ = \frac{\text{H}_2 \text{ production rate}}{\text{weight of catalyst} \times \text{volume of aqueous solution}} \end{aligned} \quad (2)$$

The apparent quantum yield (AQY) of the photocatalytic system was calculated using Equation (3). The number of incident photons was measured by the method of ferrioxalate actinometer (Montalti & Murov 2006) employing potassium ferrioxalate ($\text{K}_3[\text{Fe}(\text{C}_2\text{O}_4)_3]$).

$$\begin{aligned} \text{Apparent quantum yield} &= \frac{\text{moles of electrons reacted}}{\text{moles of incident photons}} \\ &= \frac{2 \times \text{moles of H}_2 \text{ produced}}{\text{moles of incident photons}} \end{aligned} \quad (3)$$

RESULTS AND DISCUSSION

Synthesis and characterization of the photocatalysts

Particle size distribution and morphology

Figure 1 shows the particle size distributions of the core-shell (CdS)/(ZnS) catalysts. The size of the catalysts appears independent of the catalyst composition. Such a result suggests that the particle size can be controlled by the droplet size in the microemulsion system. The catalysts ranged in size from 40 to 340 nm with a number based mean size of about 100 nm. The size measurement given by the laser particle size analyzer agrees with the SEM images of the catalysts in Figure 2. The shape and surface of the catalysts are apparently irregular. The TEM images in Figure 3 further reveal that the photocatalysts are nanoparticles with a size of around 10 nm for the primary particles. However, the nano-sized catalysts aggregated to a certain extent into larger particle clusters.

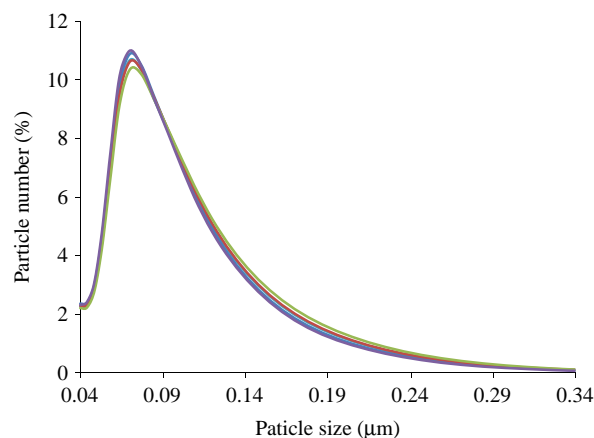


Figure 1 | Particle size distribution of the catalysts.

Photophysical properties

Figure 4(a) shows the diffuse reflectance spectra of the $(\text{CdS})_x/(\text{ZnS})_{1-x}$ core/shell catalysts. The absorption edges varied from 326 to 556 nm, and the blue shift increased as the ZnS to CdS ratio increased. Using equation $E_g(\text{eV}) = 1240/\lambda g(\text{nm})$, the absorption edges can be converted to band-gaps as shown in Figure 4(b). CdS had an intense absorption band in the visible region with a band gap of 2.23 eV. This exhibited a blue shift in the absorbance spectrum in comparison to the value (about 2.4 eV) measured for the standard bulk CdS (Bao *et al.* 2008), which is likely related to the nano-scale size of the materials (Zong *et al.* 2008). Meanwhile, $(\text{CdS})_{0.9}/(\text{ZnS})_{0.1}$ showed a band gap of 2.27 eV with both higher UV and visible absorbance values than that of CdS. When factor x varied from 0.9 to 0.1, the catalysts could be excited by visible light ($\lambda > 420$ nm) with band gaps ranging from 2.27 to 2.46 eV. The visible light absorption by the catalysts should be attributable to the CdS core.

Photocatalytic activity for H₂ production

Figure 5(a) shows hydrogen production rates for the catalysts under visible light (100 W Hg lamp, $\lambda > 420$). The photocatalytic hydrogen reactions appear to be zero order reactions during 12 h of irradiation. The hydrogen production rates for different catalysts are plotted against their compositions in Figure 5(b). The core-shell $(\text{CdS})_{0.9}/(\text{ZnS})_{0.1}$ gave the highest hydrogen production activity with

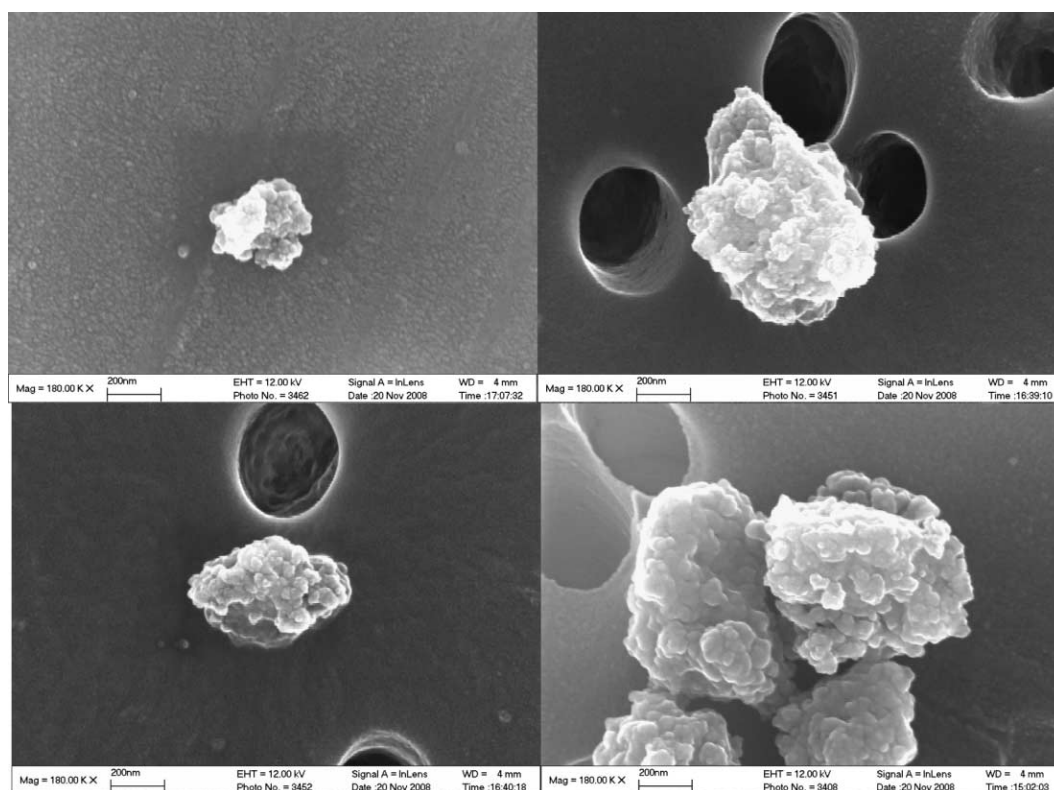


Figure 2 | SEM images of the catalysts.

a specific production rate of $21.2 \mu\text{mol h}^{-1} \text{g}^{-1}$ and a quantum yield of 5.4% under visible light. Increasing Zn content initially inhibited and then promoted the hydrogen production, reaching another peak at $x = 0.4$.

The shell of higher band-gap catalyst ZnS decreased the extent of light absorbed by the CdS core. However, the shell

could also suppress the recombination of electron and hole pairs. The higher production rate at $x = 0.9$ and 0.4 indicated the balance of these two effects. When the Zn content was lower ($x = 0.9$), an island shell of ZnS might be formed on the core, which not only separated the electrons and holes but also increased the free surface area of CdS.

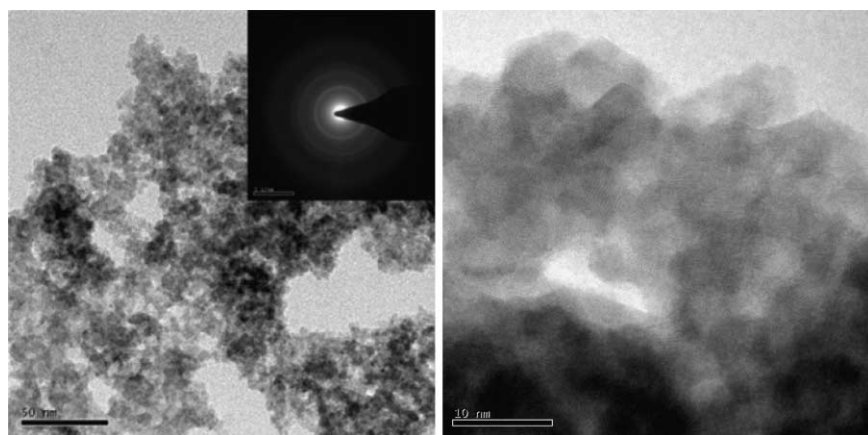


Figure 3 | TEM images of the catalysts.

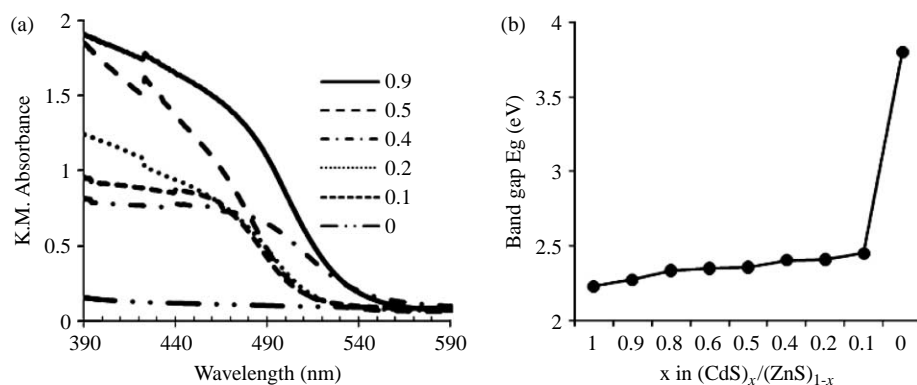


Figure 4 | Light absorption properties of the catalysts $(\text{CdS})_x/(\text{ZnS})_{1-x}$.

As the Zn content increased, a thin shell was formed; however, the band-gap of the catalyst increased due to likely the quantum effect. Thus, the electrons might not be able to overcome the barrier to the surface, resulting in a lower hydrogen production rate. When the Zn content increased further from 0.4 to 0.6, the band-gap of the catalysts did not change much but the hydrogen production rate largely increased. As Zn became further dominant in the catalyst, there were on longer enough centers of photo-excitation under visible light for hydrogen production.

The load of the catalysts in the solution also affected the performance of photo-hydrogen production (Figure 6). For catalyst $(\text{CdS})_{0.9}/(\text{ZnS})_{0.1}$, the hydrogen production rate increased initially with an increasing amount of the catalyst and then decreased as the catalyst load further increased. Meanwhile, the specific hydrogen production

rate decreased slightly when the catalyst load increased from 0.5 to 1 g/L, and it then decreased more significantly as the catalyst load increased to 1.5 g/L.

As the catalyst concentration increased, the hydrogen production rate was supposed to increase owing to more photo-excitation centers. However, the increase of solid contents in water also brought about the self-shading effect. The catalyst particles would reduce the light intensity in water by light absorption and scattering, as described by Beer-Lambert Law $I = I_0 e^{-(\epsilon_a + \epsilon_s)lC}$. The light transmission intensity decreases following an exponential function. There should be a proper catalyst load that would optimize the light transmission and the amount of catalyst particles receiving light radiation. For the reactor configuration used in this study, the optimal catalyst concentration in water was found to be 1 g/L.

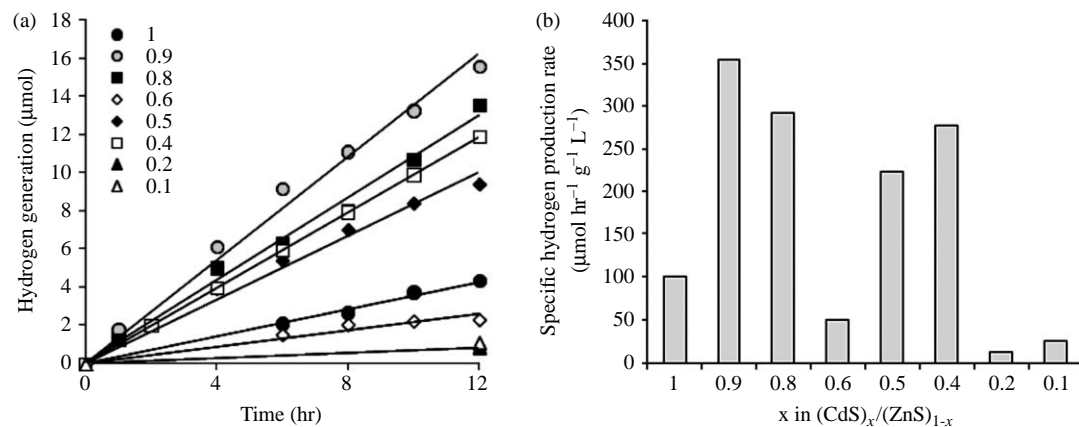


Figure 5 | Photocatalytic H_2 generation with different catalysts $(\text{CdS})_x/(\text{ZnS})_{1-x}$ under visible light (100W Hg lamp), 1 g/L catalyst in 60 ml solution containing 0.2 M Na_2SO_3 and 0.1 M Na_2S .

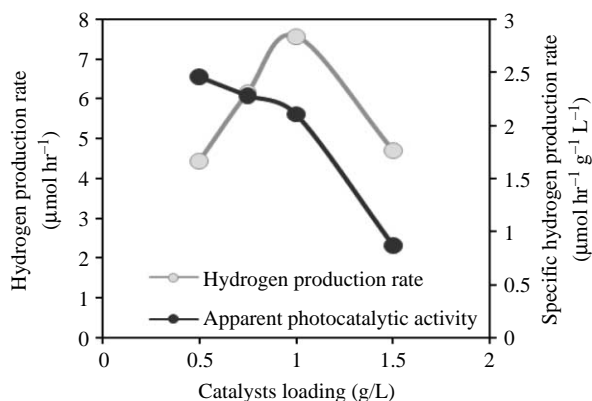


Figure 6 | The effect of the catalyst load on photocatalytic hydrogen generation by $(\text{CdS})_{0.9}/(\text{ZnS})_{0.1}$ under visible light (165W Xe lamp) in 60 ml solution containing 0.2 M Na_2SO_3 and 0.1 M Na_2S .

CONCLUSION

A series of core/shell catalysts $(\text{CdS})_x/(\text{ZnS})_{1-x}$ were synthesized using the microemulsion technique. The catalysts were characterized for their particle size distribution, UV-vis diffuse reflectance spectrum, structure and morphology. The catalysts performed well in hydrogen production from water under visible light with $\text{S}^{2-}/\text{SO}_3^{2-}$ serving as the electron donors. The highest specific hydrogen production rate was achieved at $21.2 \mu\text{mol h}^{-1} \text{g}^{-1}$ by the core/shell catalyst $(\text{CdS})_{0.9}/(\text{ZnS})_{0.1}$. The favorable feature of the nano-sized catalysts may be attributed in part to the passivation by the shell that increases the energy barrier. The core/shell structure could increase the stability of the catalysts, whilst the shell would minimize the recombination of electron/hole pairs, during the photocatalytic process. The catalyst loading density also had influence on the photo-hydrogen production rate, and the optimal catalyst concentration for the reactor cells tested was found to be 1 g/L.

ACKNOWLEDGEMENTS

This research was supported by URC funding from The University of Hong Kong and Special Equipment Grant SEG_HKU10 from the University Grants Council (UGC) of the Hong Kong SAR Government. The technical assistance of Mr. Keith C.H. Wong is highly appreciated.

REFERENCES

- Bak, T., Nowotny, J., Rekas, M. & Sorrell, C. C. 2002 Photo-electrochemical hydrogen generation from water using solar energy. Materials-related aspects. *Int. J. Hydrogen Energy* **27**(10), 991–1022.
- Bao, N. Z., Shen, L. M., Takata, T. & Domen, K. 2008 Self-templated synthesis of nanoporous CdS nanostructures for highly efficient photocatalytic hydrogen production under visible. *Chem. Mater.* **20**(1), 110–117.
- Fujishima, A. & Honda, K. 1972 Electrochemical photolysis of water at a semiconductor electrode. *Nature* **238**(5358), 37.
- Ishikawa, A., Yamada, Y., Takata, T., Kondo, J. N., Hara, M., Kobayashi, H. & Domen, K. 2003 Novel synthesis and photocatalytic activity of oxysulfide $\text{Sm}_2\text{Ti}_2\text{S}_2\text{O}_5$. *Chem. Mater.* **15**(23), 4442–4446.
- Law, M., Greene, L. E., Radenovic, A., Kuykendall, T., Liphardt, J. & Yang, P. D. 2006 $\text{ZnO-Al}_2\text{O}_3$ and ZnO-TiO_2 core-shell nanowire dye-sensitized solar cells. *J. Phys. Chem. B* **110**(45), 22652–22663.
- Lee, Y., Terashima, H., Shimodaira, Y., Teramura, K., Hara, M., Kobayashi, H., Domen, K. & Yashima, M. 2007 Zinc germanium oxynitride as a photocatalyst for overall water splitting under visible light. *J. Phys. Chem. C* **111**(2), 1042–1048.
- Maeda, K., Teramura, K., Lu, D. L., Takata, T., Saito, N., Inoue, Y. & Domen, K. 2006 Photocatalyst releasing hydrogen from water—enhancing catalytic performance holds promise for hydrogen production by water splitting in sunlight. *Nature* **440**(7082), 295.
- Montalti, M. & Murov, S. L. 2006 *Handbook of Photochemistry*. CRC/Taylor & Francis, Boca Raton.
- Tsuji, I., Kato, H., Kobayashi, H. & Kudo, A. 2004 Photocatalytic H_2 evolution reaction from aqueous solutions over band structure-controlled $(\text{AgIn})_x\text{Zn}_{2(1-x)}\text{S}_2$ solid solution photocatalysts with visible-light response and their surface nanostructures. *J. Am. Chem. Soc.* **126**(41), 13406–13413.
- Tsuji, I., Kato, H., Kobayashi, H. & Kudo, A. 2005 Photocatalytic H_2 evolution under visible-light irradiation over band-structure-controlled $(\text{CuIn})_x\text{Zn}_{2(1-x)}\text{S}_2$ solid solutions. *J. Phys. Chem. B* **109**(15), 7323–7329.
- Yu, Z. G., Pryor, C. E., Lau, W. H., Berding, M. A. & MacQueen, D. B. 2005 Core-shell nanorods for efficient photoelectrochemical hydrogen production. *J. Phys. Chem. B* **109**(48), 22913–22919.
- Zhang, K., Jing, D. W., Xing, C. J. & Guo, L. J. 2007 Significantly improved photocatalytic hydrogen production activity over $\text{Cd}_{1-x}\text{Zn}_x\text{S}$ photocatalysts prepared by a novel thermal sulfuration method. *Int. J. Hydrogen Energy* **32**(18), 4685–4691.
- Zong, X., Yan, H. J., Wu, G. P., Ma, G. J., Wen, F. Y., Wang, L. & Li, C. 2008 Enhancement of photocatalytic H_2 evolution on CdS by loading MOS_2 as cocatalyst under visible light irradiation. *J. Am. Chem. Soc.* **130**(23), 7176–7177.